

Phase-diversity phase-sensitive amplification in fiber loop with polarization beam splitter



K. Inoue

Osaka University, 2-1 Yamadaoka, Suita, Osaka 565-0871, Japan

ARTICLE INFO

Article history:

Received 23 January 2015

Revised 13 July 2015

Keywords:

Phase-sensitive amplification

Phase-diversity

Fiber parametric amplifier

ABSTRACT

In this paper, we propose a parametric amplification scheme based on phase-sensitive amplification in an optical fiber. The proposed system consists of a nonlinear fiber and a dispersive medium in a loop configuration with a polarization beam splitter, where phase-sensitive amplification occurs bi-directionally. The dispersive medium shifts the relative phase between signal and pump lights, due to which the amplified signal light is always obtained regardless of the signal input phase, i.e., a phase-diversity operation is achieved, while the output phase is digitized as in conventional phase-sensitive amplifiers.

© 2015 Elsevier Inc. All rights reserved.

1. Introduction

Phase-sensitive amplification (PSA) based on a parametric interaction between pump and signal lights has a unique property that it amplifies selective phase components while suppressing others, depending on the relative phase between the pump and signal lights [1,2]. As a result, the amplified signal has a particular phase irrespective of its input phase. This unique output property of PSA can be utilized for the phase stabilization or signal regeneration of the phase-modulated signal light. Various studies have reported PSA-based phase regeneration [3–8].

One issue in the practical implementation of PSA is phase synchronization. Because the signal gain is sensitive to the input phase, the relative phase between the pump and signal lights must be adjusted so that the signal light is amplified. Thus, a phase-locking technique is required for implementing the PSA. In order to be free from this issue, an orthogonally-pumped fiber parametric amplifier accompanied by a fiber loop with a polarization beam splitter (PBS) was recently proposed [9]. This paper suggests another PSA-based optical amplification system that outputs a phase-digitized signal light with low input-phase dependency. The proposed system consists of a nonlinear fiber and a dispersive medium in a loop configuration with a PBS; PSA occurs bi-directionally in the nonlinear fiber loop. The dispersive medium shifts the relative phase between the pump and signal lights in the two directions, and thus, signal light with an arbitrary input phase is phase-sensitively amplified in either of the two directions and the amplified signal is always obtained from the system with a digitized phase.

2. Configuration and operation mechanism

The basic configuration of the proposed scheme is shown in Fig. 1; it consists of a nonlinear fiber and a dispersive medium connected to a polarization beam splitter (PBS) in a loop configuration. Into this fiber loop, a signal and two pump lights are incident on port A of the PBS via a polarizer whose transmission axis is inclined at 45° with respect to the PBS principal axes. The polarization states of the incident lights are adjusted so that these lights pass through the polarizer. Their frequencies satisfy the condition $f_s = (f_1 + f_2)/2$, where f_s , f_1 , and f_2 are the frequencies of the signal and two pump lights, respectively, as illustrated in the inset in Fig. 1. The incident lights are decomposed into two orthogonal linear polarization states at the PBS (hereafter called the x and y polarization states). The x - and y -polarized lights are coupled out to ports C and B, respectively. The y -polarized lights travel through the nonlinear fiber in the clockwise direction, and are incident on port C of the PBS via the dispersive medium. The x -polarized lights, on the other hand, pass through the dispersive medium first, travel through the nonlinear fiber in the counterclockwise direction, and are incident on port B of the PBS. Here, the polarization state is assumed to be adjusted so that the polarization state is identical at ports B and C after propagating through the fiber loop by use of, for example, a polarization controller or a polarization maintaining fiber. Then, the x and y signal components are polarization-multiplexed and coupled out from port D at the PBS.

The behavior of all lights in the above system can be analyzed as follows. In the nonlinear fiber, a parametric interaction occurs between the signal and pump lights; this interaction can be described by the following nonlinear coupled Eq. (1):

E-mail address: kyo@comm.eng.osaka-u.ac.jp

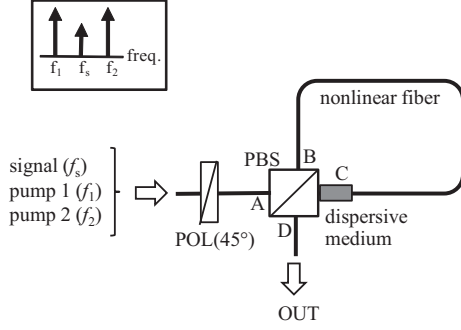


Fig. 1. Configuration of proposed phase-sensitive amplification system. PBS: polarization beam splitter, POL: polarizer, CIR: optical circulator, and PM nonlinear fiber: polarization-maintaining nonlinear fiber.

$$\frac{dE_{1,2}}{dz} = i\gamma(|E_{1,2}|^2 + 2|E_{2,1}|^2 + 2|E_s|^2)E_{1,2} + i\gamma E_s^2 E_{2,1}^* e^{-i\Delta\beta z}, \quad (1a)$$

$$\frac{dE_s}{dz} = i\gamma(2|E_1|^2 + 2|E_2|^2 + |E_s|^2)E_s + i\gamma E_1 E_2 E_s^* e^{i\Delta\beta z}. \quad (1b)$$

Here, E_s , E_1 , and E_2 are the complex amplitudes of the signal and the two pump lights, respectively; γ is the nonlinear coefficient; $\Delta\beta$ is the linear phase mismatch; and z is the propagation direction. For simplicity, the propagation loss is not taken into account. Under the small signal condition, $|E_s| \ll |E_1|, |E_2|$, the above coupled equations can be analytically solved as [1,10]:

$$E_s(L) = \{E_s(0) \cosh(2\gamma P_0 L) + i e^{i(\theta_1(0) + \theta_2(0))} E_s(0)^* \sinh(2\gamma P_0 L)\} e^{i4\gamma P_0 L}, \quad (2)$$

where $E_s(0)$ is the initial signal amplitude; P_0 is the input power of each pump light; $\theta_1(0)$ and $\theta_2(0)$ are the initial phases of the two pumps, respectively; $E_s(L)$ is the signal amplitude after propagating through length L ; and the nonlinear phase-matching condition, $\Delta\beta - 2\gamma P_0 = 0$, is assumed to be satisfied. When the pump power is sufficiently high so that $\exp(2\gamma P_0 L) \gg 1$, Eq. (2) is approximated as:

$$E_s(L) \approx \sqrt{P_s(0)} e^{2\gamma P_0 L} \cos[\theta_s(0) - \theta_p(0) - \pi/4] e^{i(\theta_p(0) + \pi/4 + 4\gamma P_0 L)}, \quad (3)$$

where $P_s(0)$ is the initial signal power, $\theta_s(0)$ is the initial signal phase, and $\theta_p(0)$ is the average of the initial pump phases, defined as $\theta_p(0) = \{\theta_1(0) + \theta_2(0)\}/2$.

In the fiber loop shown in Fig. 1, the initial states of the signal and the two pump lights in the clockwise direction can be expressed as:

$$E_s^{(cw)}(0) = \sqrt{P_{s0}/2} e^{i(\theta_{s0} + \pi/2)}, \quad (4a)$$

$$E_{1,2}^{(cw)}(0) = \sqrt{P_{p0}/2} e^{i(\theta_{10,20} + \pi/2)}, \quad (4b)$$

and those in the counterclockwise direction can be expressed as:

$$E_s^{(ccw)}(0) = \sqrt{P_{s0}/2} e^{i(\theta_{s0} + \beta_s z_d)}, \quad (5a)$$

$$E_{1,2}^{(ccw)}(0) = \sqrt{P_{p0}/2} e^{i(\theta_{10,20} + \beta_{1,2} z_d)}, \quad (5b)$$

where P_{s0} and P_{p0} are the signal and pump powers incident to the PBS, respectively; θ_{s0} , θ_{10} , and θ_{20} are the incident signal and pump phases, respectively; β_s , β_1 , and β_2 are the propagation constants for the signal and pump lights in the dispersive medium, respectively;

and z_d is the length of the dispersive medium. Applying the above initial states to Eq. (3), we obtain the signal light after traveling through the nonlinear fiber as:

$$E_s^{(cw)}(L) = \sqrt{P_{s0}/2} e^{2\gamma P_{p0} L} \cos[\theta_{s0} - \theta_{p0} - \pi/4] e^{i(\theta_{p0} + 3\pi/4 + 2\gamma P_{p0} L)}, \quad (6a)$$

$$E_s^{(ccw)}(L) = \sqrt{P_{s0}/2} e^{2\gamma P_{p0} L} \cos[\theta_{s0} - \theta_{p0} + \{\beta_s - (\beta_1 + \beta_2)/2\} z_d - \pi/4] \times e^{i(\theta_{p0} + (\beta_1 + \beta_2) z_d / 2 + \pi/4 + 2\gamma P_{p0} L)}, \quad (6b)$$

where $\theta_{p0} = (\theta_{10} + \theta_{20})/2$.

The signal lights traveling in the clockwise and counterclockwise directions are polarization-multiplexed and coupled out from port D of the PBS, which can be expressed as:

$$E_s(\text{OUT}) = \begin{pmatrix} E_s^{(ccw)}(L) \\ E_s^{(cw)}(L) e^{i(\beta_s z_d + \pi/2)} \end{pmatrix} = \sqrt{P_{s0}/2} e^{2\gamma P_{p0} L} e^{i(\theta_{p0} + \pi/4 + 2\gamma P_{p0} L)} \times \begin{pmatrix} \cos[\theta_{s0} - \theta_{p0} + \{\beta_s - (\beta_1 + \beta_2)/2\} z_d - \pi/4] e^{i(\beta_1 + \beta_2) z_d / 2} \\ \cos[\theta_{s0} - \theta_{p0} - \pi/4] e^{i(\pi + \beta_s z_d)} \end{pmatrix}. \quad (7)$$

Here, we assume $\{\beta_s - (\beta_1 + \beta_2)/2\} z_d = \pi/2$, which is not difficult to satisfy in practice [see the Appendix]. Then, the above equation can be rewritten as

$$E_s(\text{OUT}) = \sqrt{P_{s0}/2} e^{2\gamma P_{p0} L} e^{i(\theta_{p0} + \pi/4 + 2\gamma P_{p0} L)} \times \begin{pmatrix} \cos(\theta_{s0} - \theta_{p0} + \pi/4) e^{i(\beta_s z_d - \pi/2)} \\ \cos(\theta_{s0} - \theta_{p0} - \pi/4) e^{i(\pi + \beta_s z_d)} \end{pmatrix} = \sqrt{P_{s0}/2} e^{2\gamma P_{p0} L} e^{i(\theta_{p0} - \pi/4 + 2\gamma P_{p0} L + \beta_s z_d)} \times \begin{pmatrix} \cos(\theta_{s0} - \theta_{p0} + \pi/4) \\ \sin(\theta_{s0} - \theta_{p0} + \pi/4) e^{i3\pi/2} \end{pmatrix}. \quad (8)$$

The total power of this signal output is

$$|E_s(\text{OUT})|^2 = \frac{P_{s0}}{2} e^{2\gamma P_{p0} L} \{\cos^2(\theta_{s0} - \theta_{p0} + \pi/4) + \sin^2(\theta_{s0} - \theta_{p0} + \pi/4)\} = \frac{e^{2\gamma P_{p0} L}}{2} P_{s0}. \quad (9)$$

This equation suggests that amplified signal light is always outputted independent of the input phase. In addition, Eq. (8) shows that the phase of the output signal light does not depend on the signal input phase. Thus, the phase digitizing property, which is observed in conventional PSA, is obtained in our system.

Eq. (8) suggests that the cos and sin components, i.e., two quadrature components, are outputted as the x and y polarization states, respectively, meaning that the two quadrature components are demultiplexed into two cross-polarized lights. This function of quadrature-demultiplexing is achieved in a vector PSA system [11]. The present system offers the same function in a different way.

Eq. (8) also indicates that the output ratio of the two orthogonal components depends on the signal input phase with a constant phase difference between them, meaning that the output polarization state depends on the input phase. In other words, the present scheme performs phase-to-polarization conversion. This property is somewhat similar to phase-to-amplitude conversion in conventional PSAs, in a sense that it can be a drawback of degrading the signal receiver performance. Nevertheless, this drawback may be mitigated when the system operates under gain-saturated conditions, as in conventional PSAs. Further studies will be necessary for quantitative evaluation of the effect of the phase-to-polarization conversion.

3. Calculation

We carried out numerical calculations using Eq. (1) to confirm the above operation. First, the amplification characteristics under unsaturated conditions were calculated. The results are shown in Figs. 2 and 3. Considering the misalignment of the polarizer angle in the actual implementation, several angles of the polarizer with respect to the PBS principal axes were examined. Fig. 2 shows the total signal gain as a function of the signal input phase. The signal gain, which depends on the signal input phase at misaligned

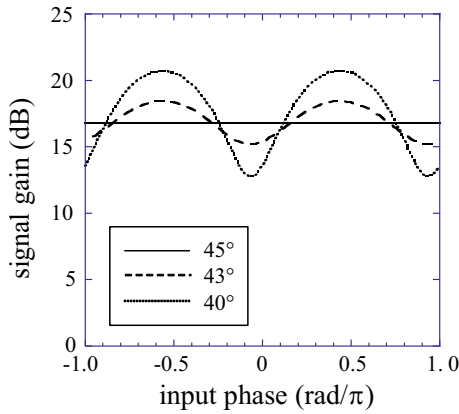


Fig. 2. Signal gain as a function of signal input phase. Signal input power is -10 dBm. The polarizer angle with respect to the PBS principal axes is 40° (dotted line), 43° (broken line), and 45° (solid line). The other parameters are $\gamma = 12 \text{ W}^{-1} \text{ km}^{-1}$; $L = 200 \text{ m}$; $P_{p0} = 0.5 \text{ W}$; and $\Delta\beta$ is a value that satisfies the nonlinear phase matching condition for a polarizer angle of 45°, i.e., $\Delta\beta - 2\gamma(P_{p0}/2) = 0$.

angles, becomes uniform at an angle of 45°, indicating signal amplification with low input-phase dependency. Fig. 3 shows the signal output power and phase for each polarization component under the same conditions in Fig. 2. It is indicated in Figs. 2 and 3 that the signal powers of the two polarization components vary in a complementary manner and, as a result, the variation in the total power turns to be small or disappears when the polarization axis is perfectly aligned. Fig. 3 also shows that the output phases of each component are quantized, such that they are mostly constant and periodically jump by π at particular input phases; the interval of these particular input phases is π . This output phase behavior is similar to that in conventional PSA. The phase jumping points are shifted by $\pi/2$ between the two polarization components, corresponding to the complementary behavior of the output powers.

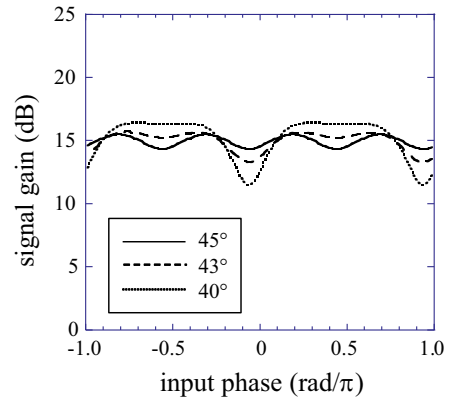


Fig. 5. Signal gain for an input power of 13 dBm. The other conditions are the same as those in Fig. 2.

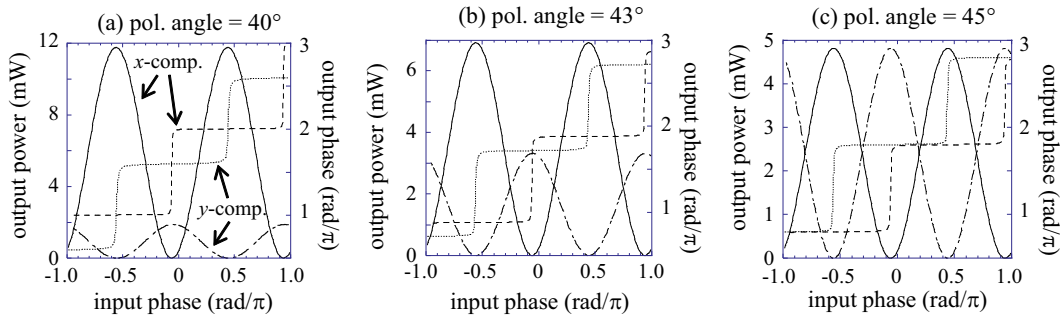


Fig. 3. Signal output power and phase for each polarization component under the conditions shown in Fig. 2. Solid and dashed lines are the gain and phase for x-polarized component, and chain and dotted lines are those for y-polarized component, respectively. The polarizer angle is 40° (a), 43° (b), and 45° (c).

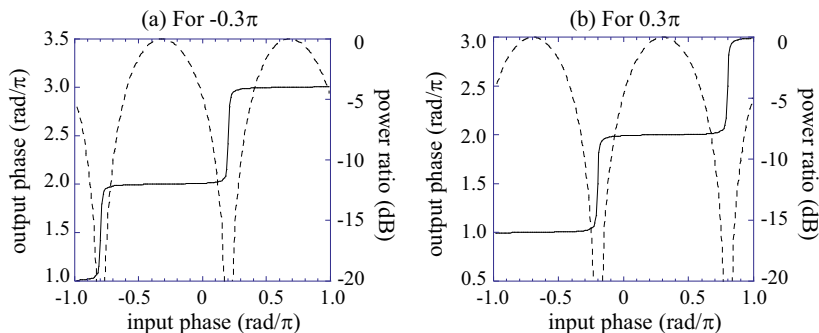


Fig. 4. Phase of output signal field in one polarization mode (solid line). Output states for input phases of -0.3π and 0.3π are chosen as the signal polarization mode in (a) and (b), respectively. The power of the signal polarization mode relative to the total power is also plotted (dashed line). The system conditions are identical to those in Fig. 3(c).

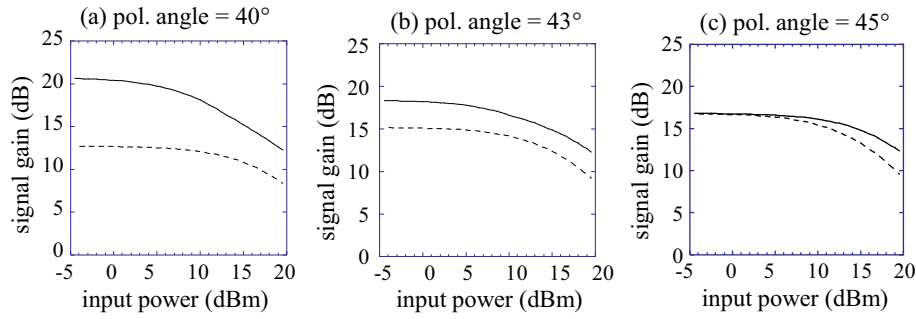


Fig. 6. The signal gain as a function of the signal input power. Solid and dashed lines are the maximum and minimum gains, respectively. The polarizer angle is 40° (a), 43° (b), and 45° (c), and the other conditions are the same as those in Fig. 2.

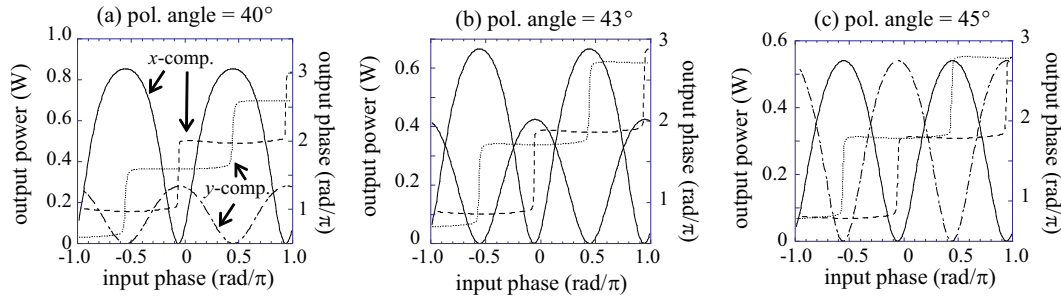


Fig. 7. Signal output power and phase for each polarization component under the conditions shown in Fig. 4. Solid and dashed lines are the gain and phase for x-polarized component, and chain and dotted lines are those for y-polarized component, respectively. The polarizer angle is 40° (a), 43° (b), and 45° (c).

It is noted that, at an input phase at which the phase of one component jumps, the corresponding output power is approximately zero and the other component is dominant with a constant phase, suggesting that the phase of the output signal is roughly independent of the input phase.

In the above, the output phases of the two orthogonal polarization components are respectively calculated. Next, we regard the output signal state as one polarization mode. This can be made by introducing the following unitary transformation in terms of the polarization coordinates.

$$\begin{pmatrix} E_p \\ E_q \end{pmatrix} = \frac{1}{\sqrt{|\bar{E}_x|^2 + |\bar{E}_y|^2}} \begin{pmatrix} \bar{E}_x^* & \bar{E}_y^* \\ \bar{E}_y & -\bar{E}_x \end{pmatrix} \begin{pmatrix} E_x \\ E_y \end{pmatrix}, \quad (10)$$

where $(E_x, E_y)^T$ the output light expressed in the polarization coordinate matched to the PBS principle axes, and \bar{E}_x and \bar{E}_y are the mean values of the x and y components, respectively. In the transformed polarization coordinate, E_p is dominant while $E_q = 0$ on average. Then, we can regard E_p as the output signal field.

Fig. 4 plots the phase of the signal field defined as above as a function of the input phase under the system conditions in Fig. 3(c). The output states for input phases of -0.3π and 0.3π are chosen as the signal polarization mode in Fig. 4(a) and (b), respectively. The signal phase is shown to be digitized as in conventional PSAs. The power of the signal polarization mode relative to the total power, $|E_p|^2/(|E_p|^2 + |E_q|^2)$, is also plotted in the figure, showing that the signal mode is dominant in the phase constant regions.

The above calculations were made for unsaturated conditions. We also examined the gain-saturated conditions. Fig. 5 shows the signal gain as a function of the input phase. The gain undulation observed for misaligned polarizer angles is reduced under gain-saturated conditions. Instead, however, some gain undulation

appears for a polarizer angle of 45°, an angle at which uniform gain is obtained under unsaturated conditions. The dependence of the gain undulation on the saturation condition is shown in Fig. 6, where the maximum and minimum gains are plotted as a function of the signal input power. The gain difference becomes small as the saturation proceeds for a misaligned polarizer angle, whereas it becomes large for an ideally aligned angle. Fig. 7 shows the output power and the phase of each polarization component as functions of the signal input power under the conditions in Fig. 5. It is noted in Fig. 7(c) that peak levels of one polarization component are depressed and, as a result, the high output power levels of one component do not fully compensate for the low levels of the other one. This property causes the gain undulation in Fig. 5 for a polarizer angle of 45°. Nevertheless, the output phase properties observed under unsaturated conditions are also obtained under gain-saturated conditions.

4. Summary

This paper proposed a parametric amplification scheme based on PSA in an optical fiber. The proposed system is composed of a nonlinear fiber loop with a dispersive medium, in which PSA occurs bi-directionally. Because of the phase shift between signal and pump lights induced in the dispersive medium, the signal light is amplified in either of the two directions and is always outputted from the system with a digitized output phase for any given input phase. Calculations using nonlinear coupled-equations confirmed the operation of the scheme.

Appendix.

The dispersive medium used in the proposed system is assumed to satisfy $\{\beta_s - (\beta_1 + \beta_2)/2\}z_d = \pi/2$. This condition can be met by,

for example, a length of normal dispersion fiber as follows. First, we expand the propagation constants at frequencies f_1 and f_2 around f_s as

$$\begin{aligned}\beta_1 &= \beta(f_s) + \frac{d\beta}{df}(f_1 - f_s) + \frac{1}{2} \frac{d^2\beta}{df^2}(f_1 - f_s)^2 \\ &= \beta_s - \frac{2\pi}{v_g} \Delta f - \frac{1}{2} \cdot \frac{\lambda^2 D_c}{2\pi c} (2\pi)^2 (\Delta f)^2,\end{aligned}\quad (\text{A1a})$$

$$\beta_2 = \beta_s + \frac{2\pi}{v_g} \Delta f - \frac{1}{2} \cdot \frac{\lambda^2 D_c}{2\pi c} (2\pi)^2 (\Delta f)^2 \quad (\text{A1b})$$

where $\Delta f = (f_s - f_1) = (f_2 - f_s)$; v_g is the group velocity at f_s ; λ is the signal wavelength; c is the light velocity; and D_c is the dispersion parameter of the fiber. Using these expressions, the condition required for the dispersive medium can be rewritten as:

$$\{\beta_s - (\beta_1 + \beta_2)/2\}z_d = \frac{\pi\lambda^2 D_c}{c} (\Delta f)^2 z_d = \frac{\pi}{2} \quad (\text{A2})$$

Using the parameters of $\lambda = 1.5 \mu\text{m}$, $D_c = 17 \text{ ps/km-nm}$, and $\Delta f = 1 \text{ THz}$, this condition is satisfied for a length of $z_d = 4 \text{ m}$.

References

- [1] C.J. McKinstrie, S. Radic, *Opt. Express* 12 (2004) 4973–4979.
- [2] Z. Tong, C. Lundström, P.A. Andrekson, M. Karlsson, A. Bogris, *IEEE J. Sel. Top. Quant. Electron* 18 (2012) 1016–1032.
- [3] A. Bogris, D. Syvridis, *IEEE Photon Technol. Lett.* 18 (2006) 2144–2146.
- [4] K. Croussore, *IEEE J. Sel. Top. Quant. Electron.* 14 (2008) 648–658.
- [5] A. Fragkos, A. Bogris, D. Syvridis, *IEEE Photon Technol. Lett.* 22 (2010) 1826–1828.
- [6] P. Frascella, S. Sygletos, F. Garcia Gunning, R. Weerasuriya, L. Grüner-Mielsen, R. Phelan, J. O’Gorman, A. Ellis, *IEEE Photon. Technol. Lett.* 21 (2011) 516–518.
- [7] M.A. Ettabib, F. Parmigiani, X. Feng, L. Jones, J. Kakande, R. Slavík, F. Poletti, G.M. Ponzio, J. Shi, M.N. Petrovich, W.H. Loh, P. Petropoulos, D.J. Richardson, *Opt. Express* 20 (2012) 27419–27424.
- [8] R. Slavík, A. Bogris, F. Parmigiani, J. Kakande, M. Westlund, M. Sköld, L. Grüner-Nielsen, R. Phelan, D. Syvridis, P. Petropoulos, D. Richardson, *IEEE J. Sel. Top. Quant. Electron.* 18 (2012) 859–869.
- [9] K. Inoue, *Opt. Express* 23 (2015) 3440–3447.
- [10] M. Vasilyev, *Opt. Express* 13 (2005) 7563–7571.
- [11] A. Lorences-Riesgo, L. Liu, S. Olsson, R. Malik, A. Kumpera, C. Lundström, F. Chiarello, S. Radic, M. Karlsson, P.A. Andrekson, *Opt. Express* 22 (2014) 29424–229434.